

Short Communication

A comparison of the Electrochemical Properties of graphene/Mn₃O₄ Composites fabricated by two Different Methods

Hoda Nourmohammadi Miankushki, Arman Sedghi*, Saeid Baghshahi

Department of Materials Science and Engineering, Faculty of Engineering, Imam Khomeini International University, Qazvin, 34149-16818, Iran

*E-mail: sedghi@eng.ikiu.ac.ir

Received: 12 November 2017 / *Accepted:* 6 January 2018 / *Published:* 5 February 2018

In this study, graphene/Mn₃O₄ composites were fabricated to improve the specific capacitance of graphene based supercapacitor, using two different simple methods. First, Graphene/Mn₃O₄ composite (GM1) was synthesized through deposition of nanoscale manganese oxide on the surface of graphene under microwave irradiation. Second, a two-step method consisting of mixing and annealing was employed to fabricate graphene/Mn₃O₄ composite (GM2). The prepared materials were characterized by X-ray diffraction (XRD), field emission scanning electron microscopy (FESEM) and Fourier transform infrared spectroscopy (FT-IR). The XRD analysis revealed the formation of graphene/Mn₃O₄. Moreover, the presence of Mn₃O₄ and MnO₂ was conformed using Fourier transform infrared spectroscopy. GM2 electrode showed better electrochemical performance, and exhibits the largest specific capacitance of approximately 100 F/g at the scan rate of 30 mv/s in 1 M H₂SO₄ electrolyte. In addition, other electrochemical measurements of the electrodes were implemented proposing that the graphene/Mn₃O₄ composite electrodes are promising materials for supercapacitor application.

Keywords: Graphene, Mn₃O₄, Composites, supercapacitor

1. INTRODUCTION

Supercapacitors are a new type of energy storage devices that have properties between batteries and electrostatic capacitors [1]. There are two kinds of supercapacitors that are differentiated according to the charge-storage mechanisms. In electrical double layer capacitors, charge is stored by adsorption/desorption of electrolyte ions on surface of carbon materials. In pseudocapacitors, charge is stored by Faradaic reactions in metal oxide or conducting polymer. [2] For improving supercapacitors properties it is possible to combine carbon materials with metal oxides or conducting polymers.

Among carbon materials, graphene has been very much considered because of their unique morphology, chemical stability and good electrical conductivity. Currently, the combination of metal oxides with graphene has been considered as an effective way to improve the electrochemical properties of graphene electrodes. [3-9]. In general, the metal oxides applied for SCs include RuO₂ [3], IrO₂ [4], MnO₂ [5], Mn₃O₄ [6], Co₃O₄ [7], and NiO [8], Among these metal oxides Manganese oxides (MnO_x) are thought to be competitive to incorporate with graphene because of their high industrial yields, low cost, low price, and non-toxicity. Mn element has different chemical valence (Mn²⁺, Mn³⁺, and Mn⁴⁺), so there are different manganese oxides, such as MnO, MnO₂, Mn₂O₃, and Mn₃O₄. Among them, Mn₃O₄ as a mixed valence MnO_x are very suitable for supercapacitors application [9-12].

Different researchers have been investigated graphene/MnO_x based electrodes [13-20]. A typical synthesis procedure can be summarized as a two-step method: synthesis of graphene and deposition of MnO_x on graphene. For instance, Jun Yan et al and Liu et al [17, 18] prepared the capacitive graphene/MnO₂ and graphene/Mn₃O₄ by deposition of nanoscale manganese oxide on the surface of as prepared graphene under microwave irradiation and they exhibited the Cs of 310 F g⁻¹ at 2 mV s⁻¹ in 1 M Na₂SO₄ and 193 F g⁻¹ at 25 mV s⁻¹ in 0.5 M Na₂SO₄ electrolyte respectively. Meanwhile, through a mixing and annealing synthesis strategy, Y. Yang et al and Wang et al [15,19] synthesized graphene/MnO₂ and graphene/Mn₃O₄ composite and the Cs of composites reached to 450 F g⁻¹ at 1A/g and 256 F g⁻¹ at 5 mV s⁻¹ in 6 M KOH electrolyte. In addition, Y. F. Liu et al, fabricated graphene/Mn₃O₄ by solvothermal method and this electrode showed 245 F g⁻¹ at 5 mV s⁻¹ in the 6M KOH solution. [20] Moreover other methods such as sonochemical method [21], hydrothermal routes [22], and chemical synthesis method [23] have been used. Between these methods, microwave and mixing-annealing requires noncomplex apparatus and simple operation. Herein, we report the preparation of graphene/Mn₃O₄ composites via two different method microwave and mixing-annealing. The properties of graphene/manganese oxide composites were investigated by X-ray diffraction (XRD), Fourier transform infrared spectroscopy (FTIR) and field emission scanning microscopy (FESEM). The as-prepared graphene/Mn₃O₄ composites with mixing – annealing method present high electrochemical performance.

2. EXPERIMENTAL

For fabrication of graphene/manganese oxide electrodes, Graphene powder was obtained from XG sciences, manganese acetate (Mn(CH₃COO)₂·4H₂O), potassium permanganate were purchased from Merck. Acetone, ethanol, distilled water. The graphite plate (1cm×2cm) was used as the current collector.

2.1. Preparation of graphene/Mn₃O₄ composite by microwave method (GMI)

Graphene/Mn₃O₄ composite were prepared by redox reaction between graphene and potassium permanganate under microwave irradiation. In the first step, 100 mL of graphene water suspension (0.165 g in 100 ml) was subjected to ultrasonic vibration for 1 h. Then KMnO₄ powder (1.15 g) was

added into above graphene suspension and stirred for 10 min. then, the resulting suspension was heated by household microwave oven (Haier, 2450 MHz, and 700 W) for 5 min, and then cooled to room temperature naturally. Finally, the suspension was filtered and black deposit was washed several times with distilled water and alcohol, and dried at 100 °C for 12 h in a vacuum oven (Fig. 1).

2.2. Preparation of graphene/Mn₃O₄ composite by mixing and annealing method (GM2)

Fifty milligrams of graphene was dispersed in 100 mL ethanol with ultrasonication for 1 h to make a graphene suspension. Then 350 milligrams of Mn(CH₃COO)₂·4H₂O was added into the graphene suspension and stirred by magnetic stirring for 1 h at 90°C and dried. Finally, the graphene/manganese oxide composite was annealed at 300°C at a rising rate of 5°C /min for 3 h in argon atmosphere. (Fig. 1)

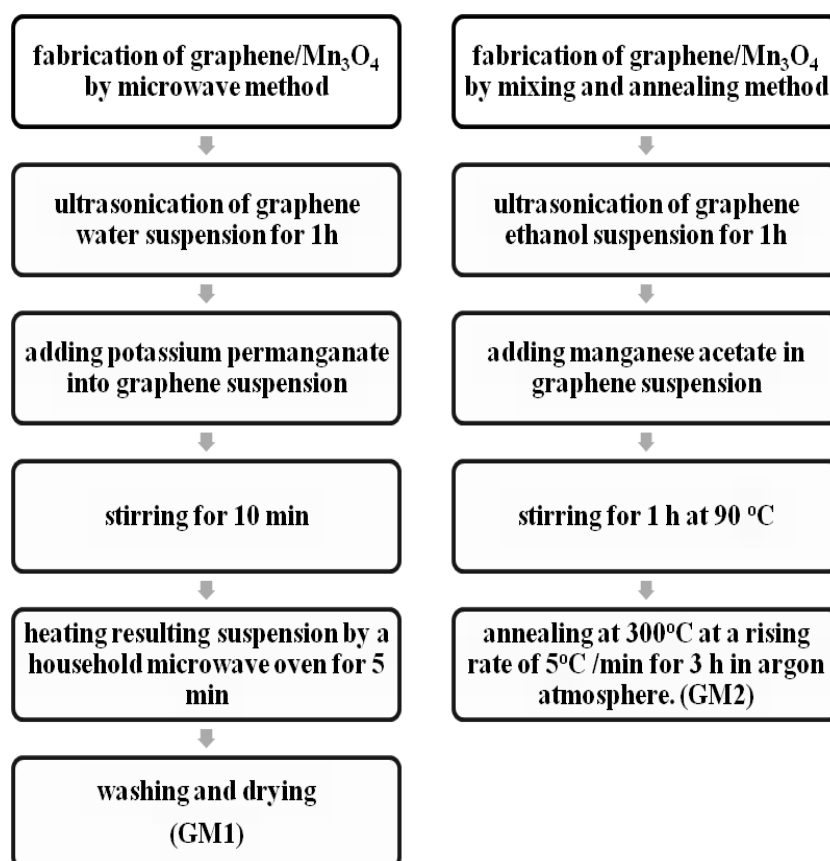


Figure 1. Flow chart of fabrication steps of graphene/Mn₃O₄ composites

2.3. Characterization and electrochemical measurements

The X-ray diffraction analysis (PHILIPS, PW1730) with a Cu-K α radiation and The Fourier transform infrared spectra (Bruker TENSOR 27 FT-IR spectrophotometer) were introduced to analyses the phase formation and element in the composites.

The surface morphology of electrodes were analyzed by field emission scanning electron microscopy (MIRA 3 TESCAN). The electrochemical experiments consist of cyclic voltammetry, galvanostatic charge-discharge and electrochemical impedance spectra (EIS) were carried out using VSP-300-Biologic multichannel potentiostat/galvanostate system with a standard three electrode system. Capacitive behavior and EIS of the films were investigated in 1 M H₂SO₄ aqueous electrolyte. For the electrochemical measurements all the electrodes were prepared by mixing the active material with PVDF to form a slurry. Then the slurry was cast on graphite plate, and dried under vacuum at 70°C for 24 h.

In three electrode system, cyclic voltammetry studies were performed within a potential range of 0 V to 1 V at different scan rate of 30 mv/s. The specific capacitance obtained by CV measurement was calculated by using the equation.1

$$C = \frac{\int I dv}{SR \times m \times \Delta v} \quad (1)$$

Where, I is current density (A/Cm²), V is potential (V), SR is scan rate (V/S) and m is the deposited weight of the material on electrode (g). Moreover the average energy density (E) and the power density (P) of the nanocomposite were evaluated from the following expressions [24]:

$$E = \frac{1}{2} C(\Delta V)^2 \quad (2)$$

Where C, ΔV and t represent the specific capacitance (F g⁻¹), the potential window (V) and discharge time (s), respectively.

Also, galvanostatic charge-discharge tests were performed at 1 A/g with a potential window of 0 to 1 V. EIS measurements were carried out by applying an AC voltage in a frequency range from 0.01 Hz to 100 kHz at an open circuit potential condition.

3. RESULTS AND DISCUSSION

The XRD patterns of graphene, GM1 and GM2 composites are shown in Fig. 2. For graphene, two diffraction peaks at 26.3° and 43° corresponds to the graphite-like structure [24]. For GM2 composite in comparison with graphene spectrum, we can see different new peaks that corresponded to Mn₃O₄. The positions can be indexed perfectly and matches well with the reported Mn₃O₄ tetragonal structure (JCPDS No. 00-001-1127). Any other impurity was not revealed in XRD results which indicates the high phase purity of the prepared samples [25, 26]. According to the XRD pattern of GM1, it is concluded that a mixed phase of Mn₃O₄ and MnO₂ are present in the prepared nanocomposite, in addition of manganese oxide peaks, it can be seen that a new peak of impurity around 50° corresponds to the K₂Mn₄O₈ [27].

FT-IR spectrums of samples are shown in Fig. 3. For the graphene/manganese oxide composites, the peaks around 400-700 cm⁻¹ are assigned to Mn-O bands. In GM2 composite, the peaks at 485 cm⁻¹ and 595 cm⁻¹ are attributed to tetrahedral and octahedral Mn-O bands, suggesting that Mn₃O₄ was bounded to the surface of graphene sheets [19].

In the spectrum of GM1 composite, Mn-O vibration modes are identified from bands between 500 cm^{-1} and 700 cm^{-1} [28].

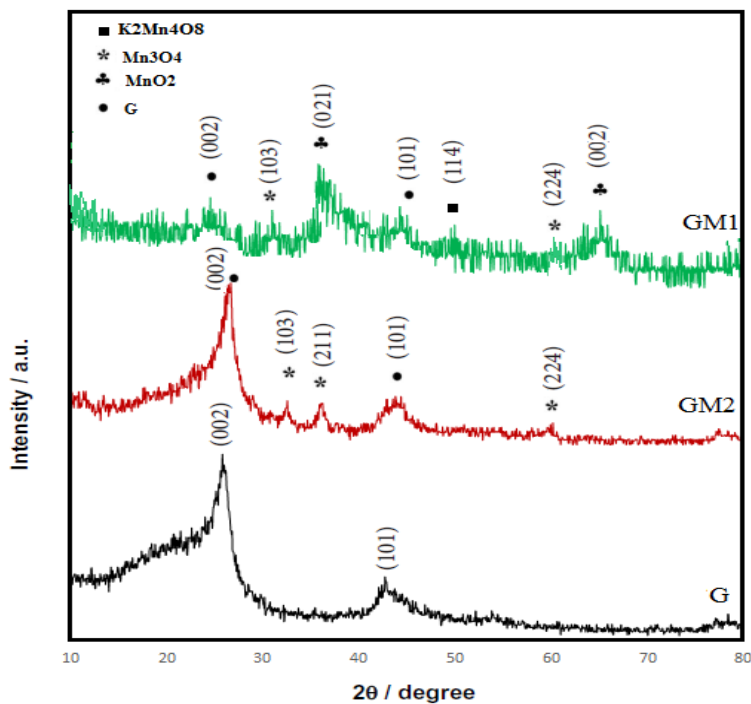


Figure 2. XRD patterns of graphene, GM1 and GM2 composites

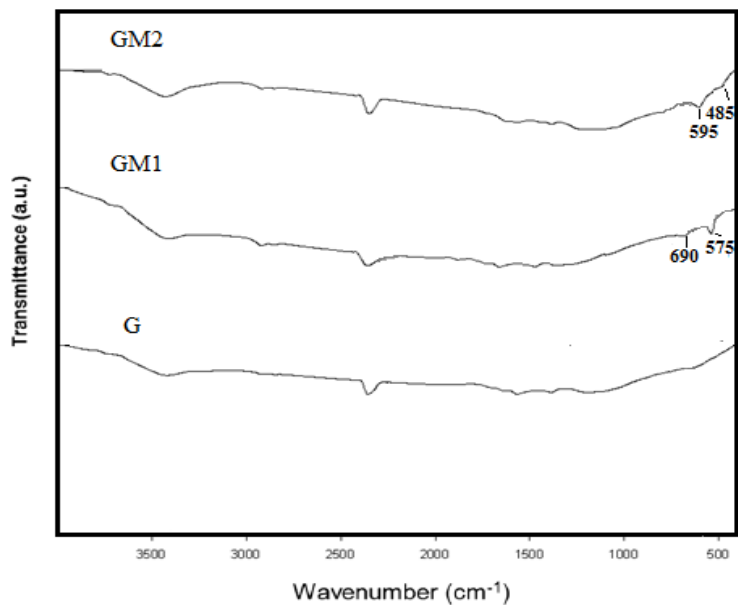
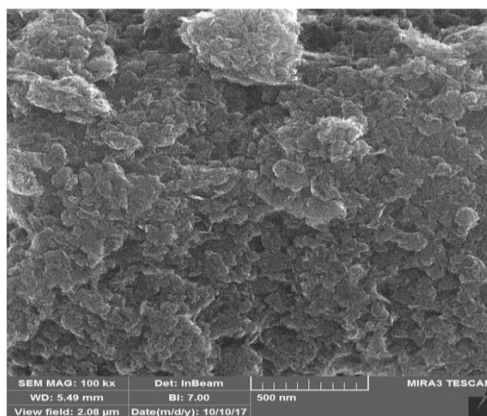


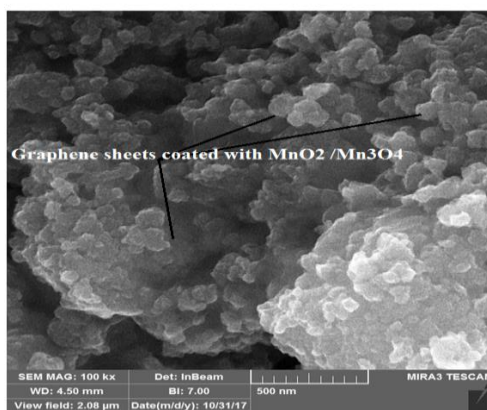
Figure 3. FTIR spectrums of graphene, GM1 and GM2 composites

Fig. 4 demonstrates the field emission scanning electron micrographs of graphene, GM1 and GM2 thin films deposited on graphite substrate. From the micrographs, it is seen that the surface morphology of graphene sheets changes from compact nanosheets to porous morphology of G/Mn₃O₄

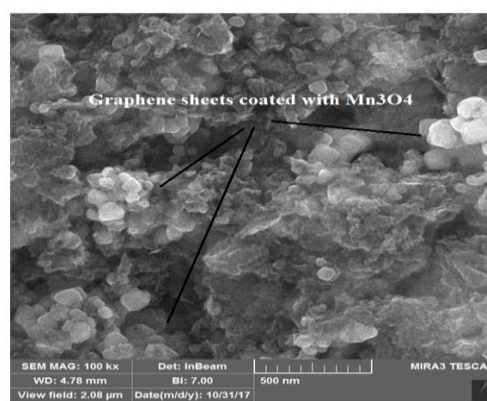
composite by the interconnection of nanosheets covered with nanograins. These nanograins have irregular shape, and randomly distributed. Porous network formed by deposition of nanograins on graphene sheets is feasible for supercapacitor application, because it can improve surface area. [23]



(a)



(b)

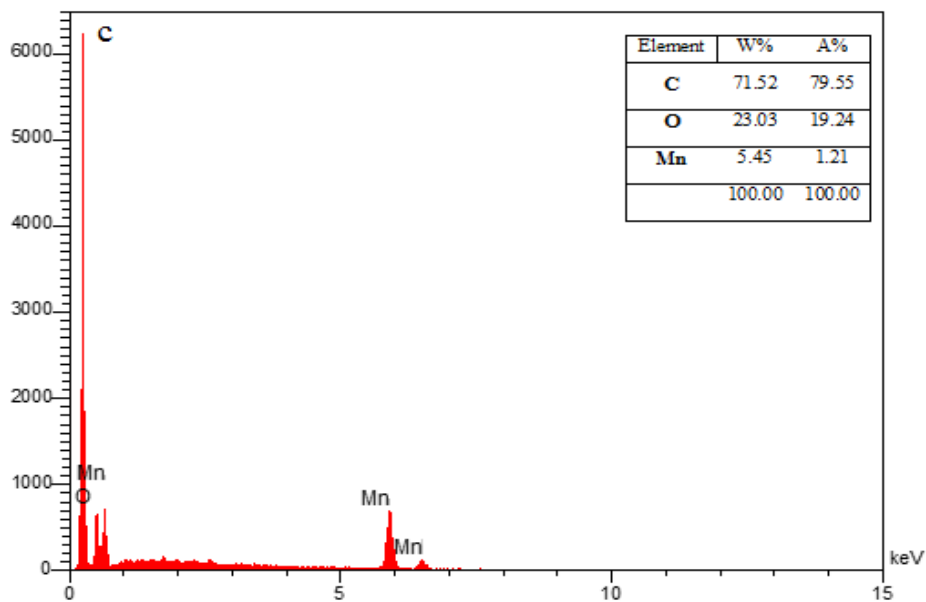


(c)

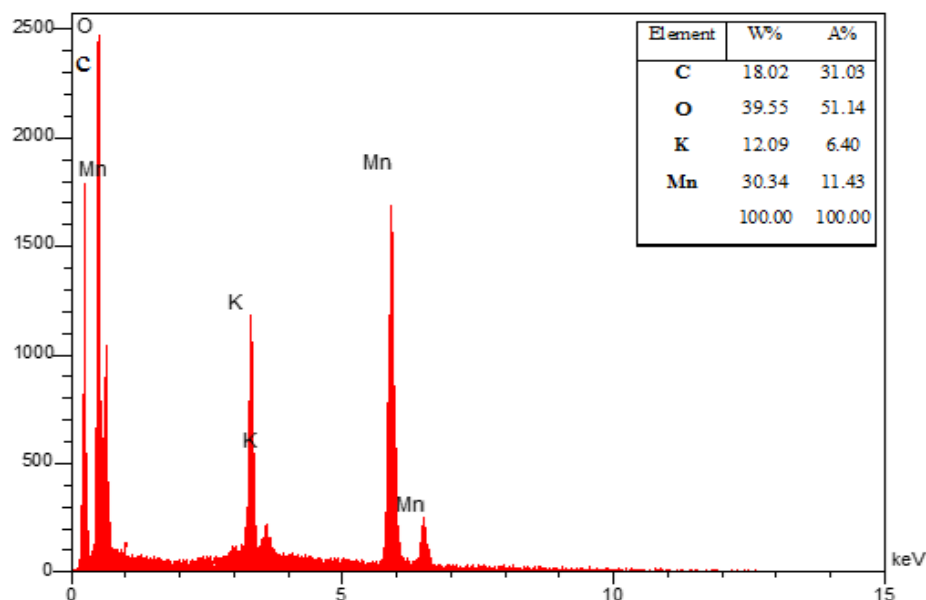
Figure 4. FESEM image of (a) graphene, (b) GM1 and (c) GM2 composites (100KX)

Fig. 5 shows the Energy dispersive spectroscopy (EDS) examination of prepared graphene/manganese oxide nanocomposites electrode. The peaks for C, O, Mn, and k elements were seen in the EDS spectrums. For the GM1, The weight percent of C, O and Mn are 18.02%, 39.55% and 30.34%, respectively. In addition from GM1 spectrum, it can be seen that the potassium energy line

with weight percent of 12.09% that conform the results of XRD. Moreover from the EDS spectrum of GM2, The weight percent of C, O and Mn are 71.52%, 23.03% and 5.45% and These results are in agreement with XRD and FTIR



(a)



(b)

Figure 5. Chemical composition of (a) GM2 and (b) GM1 samples derived from Energy dispersive spectroscopy examination under FESEM

Electrochemical tests were characterized using a three-electrode configuration, and carried out with cyclic voltammetry, galvanostatic charge/discharge and impedance measurements.

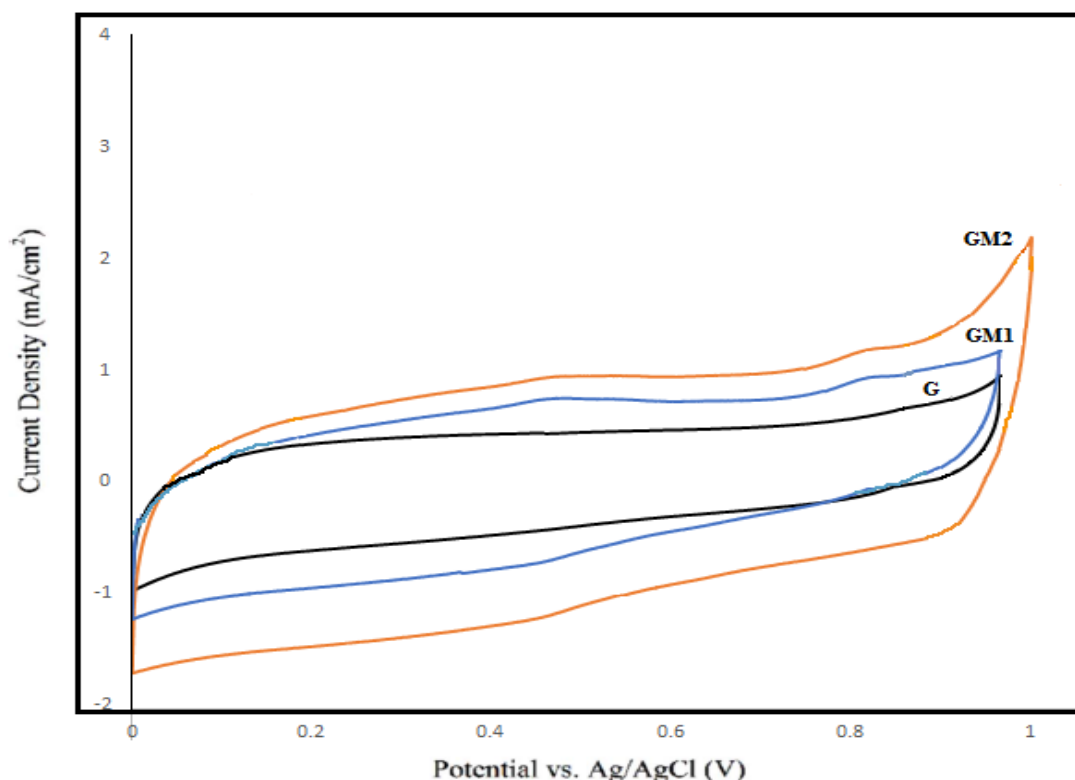
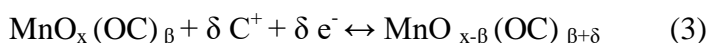


Figure 6. CV curves of graphene, GM1 and GM2 electrodes in 1M H₂SO₄ electrolyte at scan rate of 30 mV/s

As shown in Fig. 6, the shape of CV curves for graphene presents as an approximate rectangle without any redox peaks that implying graphene performed the EDLC capacitance [13]. In contrast, two pairs of redox peaks are observed in the CV curves of graphene/manganese oxide composites that demonstrating their pseudocapacitive behavior. [17] The pseudocapacitance mechanism of manganese oxides in aqueous solution is proposed by Reaction 3:



Where $\text{MnO}_x(\text{OC})_\beta$ and $\text{MnO}_{x-\beta}(\text{OC})_{\beta+\delta}$ indicate interfacial manganese oxide under the higher and lower oxidation states, respectively.[29]

Besides, CV curve of GM2 composite enclose much more areas than those of pure graphene and GM1 composite do at the same scan rate of 30 mV s⁻¹, indicating the higher Cs of GM2 composite [6].

In this investigation, cyclic voltammetry measurement of graphene, GM1 and GM2 electrodes showed the specific capacitance of 40, 66, and 100 F g⁻¹ at 30 mV s⁻¹ scan rate, respectively. The enhancement of GM2 composite capacitance is probably ascribed to the structure of graphene/Mn₃O₄ composite: (1) extra EDLC capacitance of graphene could be utilized due to the decrease of

agglomeration by the deposition of Mn_3O_4 nanoparticles; (2) high conductive graphene could improve the electrical conductivity of composite and facilitating electrons accessible to most Mn_3O_4 during charge and discharge processes; (3) Mn_3O_4 particles are in nano size and improve the amount of Mn_3O_4 /electrolyte contact areas for the redox reaction [30].

Electrochemical impedance spectra (EIS) of the graphene, GM1 and GM2 electrodes in 1 M H_2SO_4 solution are exposed in Fig. 7.

All the EIS spectra are combinations of an approximate semicircle in high frequencies and a straight line in low frequencies. The bulk solution resistance R_s can be obtained from the Nyquist plot, where the high frequency semicircle intercepts the real axis and the diameter of the semicircle corresponded to the value of the contact interface resistance R_{ct} . Moreover, the almost linear vertical line across the x-axis of the higher resistivity region implies a nearly ideal capacitive behavior for the nanocomposite, and the steeper sloped line indicates the fast diffusion of the electrolyte ions [31-33]. The value of R_s and R_{ct} of samples are shown in table.1. The EIS results show the GM2 electrode has a lower bulk solution resistance and contact interface resistance than GM1 electrodes.

Table 1. Electrochemical properties of graphene, GM1 and GM2 electrodes in 1M H_2SO_4 electrolyte at scan rate of 30 mV/s

sample	Current collector	Specific capacitance(F/g)	Energy density(W.h/Kg)	$R_s(\Omega)$	$R_{ct}(\Omega)$
graphene	graphite	40	5.56	2.5	0.01
GM1	graphite	66	9.17	3.1	0.8
GM2	graphite	100	13.89	2.7	0.2

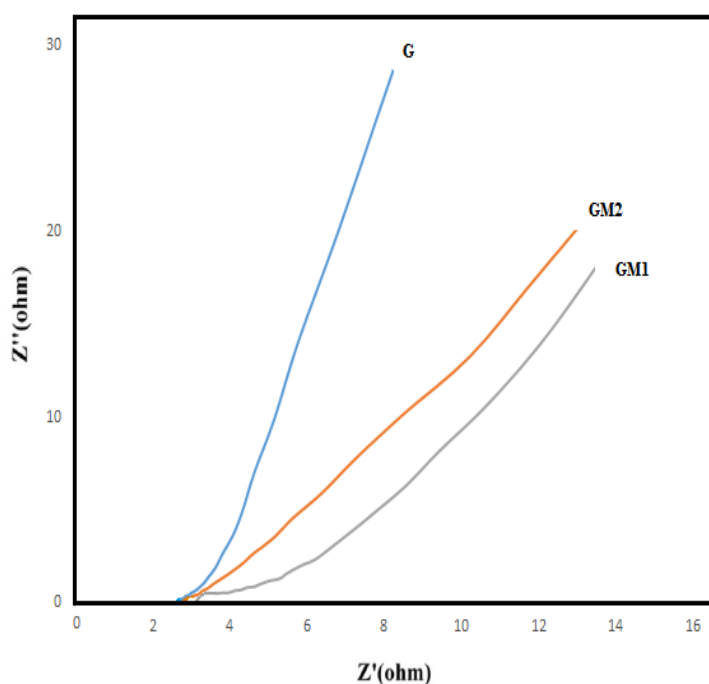


Figure 7. (a) CVs and (B) EIS of graphene, GM1 and GM2 in 1M H_2SO_4 electrolyte in a frequency range from 0.01 Hz to 100 kHz

The charge/discharge of electrodes were investigated at current densities of 1 A/g, as shown in Fig.8. It can be seen that all the curves are highly linear and symmetrical. This implies that the electrodes have excellent electrochemical reversibility and charge–discharge properties. Moreover, the IR drops on all curves are similar and not obvious, indicating little overall resistance and excellent capacitive properties of this hybrid material.[17] Compared with graphene, the composite electrodes exhibited longer discharge times at the same current density that attribute to the higher capacitance of these electrodes.

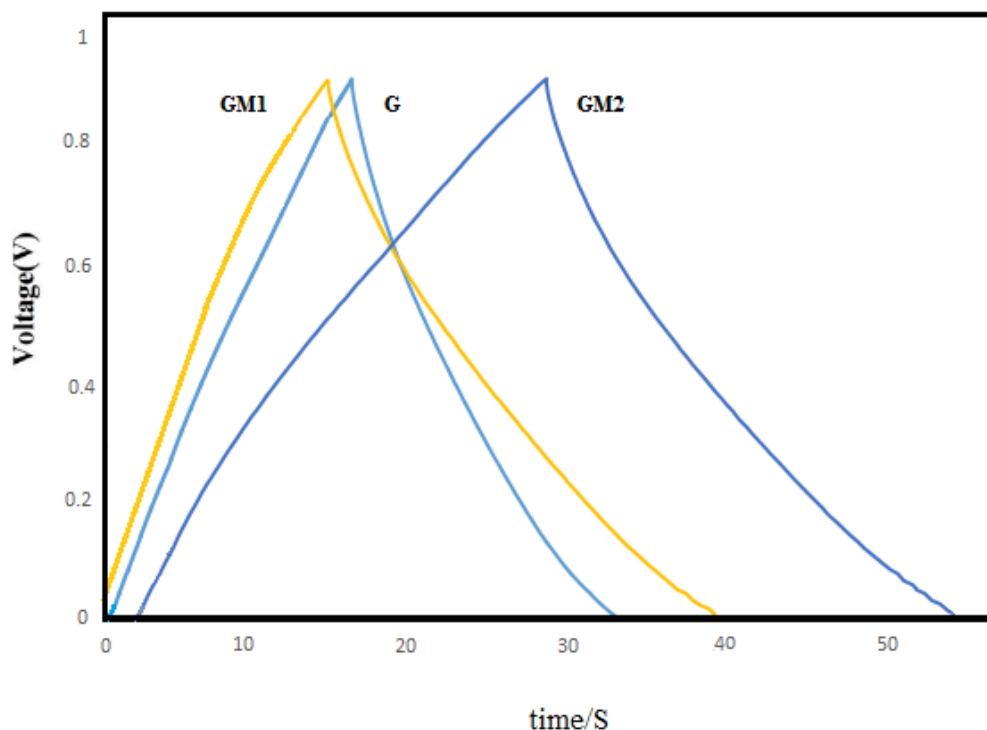


Figure 8. Charge/discharge curves of graphene, GM1 and GM2 electrodes in 1M H₂SO₄ electrolyte

Table 2 shows the comparison between the performances of our electrode in this work and those reported before. According to the contents of the table, G/Mn₃O₄ composites have been synthesized using different methods such as hydrothermal, solvothermal and so on. In comparison with our study, in solvothermal and hydrothermal methods more starting materials have been used. Moreover the solvents for preparing Mn₃O₄ with these methods often are dimethyl sulfoxide [34], methyl alcohol [35], ethylene glycol [25, 22], N, N'-dimethylformamide [36], and so forth. But in our method we used ethanol as solvent due to its low price and nontoxicity [37].

In addition the comparison shows that our G/Mn₃O₄ electrode with low cost graphite paper as current collector can compete with electrodes with other current collectors. All suggest the G/Mn₃O₄ electrode are promising electrode materials for supercapacitors.

Table 2. comparison between this work product and other reports

Basic synthesis information	Current collector	electrolyte	Specific capacitance(F/g)	Ref
GO + KMnO ₄ + H ₂ O +hydrazine hydrate, hydrothermal 453K for 6 h	Nickel foam	1M Na ₂ SO ₄	171	17
GO + (Mn(CH ₃ COO) ₂ ·H O) +KMnO ₄ +ethylene glycol +NaOH +... Hydrothermal 453 K for 5 h	Nickel foam	1M Na ₂ SO ₄	194	25
GO + Mn(CH ₃ COO) ₂ ·4H ₂ O+ dimethyl sulfoxide solvothormal 393 K for 24 h	Nickel foam	1M Na ₂ SO ₄	147	34
G+(Mn(CH ₃ COO) ₂ ·H ₂ O)+KMnO ₄ +ethanol Mixing and heating at 351 k for 2 h	Nickel foam	5M KOH	140	38
arc discharge method	Copper foil	BminBF ₄ /AN	38	39
GO + KMnO ₄ + H ₂ O +hydrazine hydrate+ ethylene glycol hydrothermal 393K for 4 h	Nickel foam	1 M Na ₂ SO ₄	88	22
G+(Mn(CH ₃ COO) ₂ ·H ₂ O) +ethanol Thermal decomposition 573 k for 3 h	graphite	1 M H ₂ SO ₄	100	This work

4. CONCLUSION

1. graphene/manganese oxides were prepared successfully by two different method: self-limiting deposition under microwave irradiation (GM1) and mixing/annealing (GM2) .The structure and morphology of these composites together with pure graphene were fully characterized with different techniques including FTIR, XRD and FESEM-EDS.

2. graphene/manganese oxides were deposited on graphite as current collector and electrochemical properties of electrodes were investigated.

3. Cyclic voltammetry and other electrochemical measurements showed that Synergistic effect between graphene and manganese oxide and improving contact surface cause to improving electrochemical properties of graphene/manganese oxide electrodes.

4. High specific capacitance was achieved for GM2 electrode with the highest specific capacitance of 100 F g⁻¹ and energy density of 13.89 Wh/Kg.

5. The results showed that, mixing and annealing method is a simple and inexpensive method for fabrication of graphene/manganese oxide composite and it is possible to fabricate good electrode for supercapacitor application.

References

1. M. Vangari, T. Pryor and L. Jiang, *J. Energy Eng.*, 130(2013).

2. R. Dong, Q. Ye, L. Kuang, X. Lu, Y. Zhang, X. Zhang, G. Tan, Y. Wen and F. Wang, *ACS Appl. Mater. Interfaces*. 5 (2013) 9508.
3. J. P. Zheng, P. J. Cygan, and T. R. Jow, *J. Electrochem. Soc.*, 142(1995)2699.
4. C.-C. Hu, Y.-H. Huang, and K.-H. Chang, *J. Power Sources*, 108(2002) 117.
5. G. Zhu, H. J. Li, L. J. Deng, and Z. H. Liu, *Mater. Lett.* 64(2010)1763.
6. D. P. Dubal, D. S. Dhawale, R. R. Salunkhe, V. J. Fulari, and C.D. Lokhande, *J. Alloys Compd.*, 497(2010) 166.
7. T.-C. Liu, W. G. Pell, and B. E. Conway, *Electrochim. Acta.* , 44(1999) 2829.
8. C. Yuan, X. Zhang, L. Su, B.Gao, and L. Shen, *J. Mater. Chem. A*, 19(2009)5772.
9. X. Lang, A. Hirata, T. Fujita and M. Chen, *Nat. Nanotechnol.* 6(2011), 232.
10. S.W. Zhang, G.Z. Chen, *Energy Mater.* , 3 (2008), 186.
11. K. Takahashi, *Electrochim. Acta* 26(1981), 1467.
12. K.H. Chang, Y.F. Lee, C.C. Hu, C.I. Chang, C.L. Liu, Y.L. Yang, *Chem. Commun*,46(2010) ,7957.
13. J. Yan, Z. Fan, T. Wei, W. Qian, M. Zhang, F. Wei, *Carbon* 48(2010), 3825.
14. S. Chen, J. Zhu, X. Wu, Q. Han, X. Wang, *ACS Nano* 4(2010), 2822.
15. H. Wang, Q. Hao, X. Yang, L. Lu, X. Wang, *Electrochem. Commun.* 11(2009), 1158.
16. Q. Cheng, J. Tang, J. Ma, H. Zhang, N. Shinya, L.C. Qin, *Carbon* 49(2011) ,2917.
17. Lingxiang Zhu, Su Zhang, Yuhua Cui, Huaihe Song, Xiaohong Chen, *Electrochim. Acta*, 89(2013), 18– 23.
18. C.L. Liu, K.H. Chang, C.C. Hu, W.C. Wen, *J. Power Sources*, 217(2012), 184.
19. Y. Yang, B. Zeng, J. Liu¹, Y. Long, N. Li, Z. Wen and Y. Jiang, *Mater.Res.Innovations*, 20 (2015).
20. Y. F. Liu, G. H. Yuan, Z. H. Jiang, and Z. P. Yao¹, *J. Nanomater.* (2014).
21. L. Wang, Y. Li and Z. Han, *J. Mater. Chem. A*, 1(2013) 8385.
22. J.W. Lee, A. S. Hall, J.-D. Kim, and T. E. Mallouk, *Chem. Mater*, 24(2012) 1158.
23. G. S. Gund, D. P. Dubal, B. H. Patil, S. S. Shinde, and C. D. Lokhande, *Electrochim. Acta*, 92(2013) 205.
24. T. Kuilla, S. Bhadra, D. Yao, N.H. Kim, S. Bose, J.H. Lee, *J. Prog. Polym. Sci*, 35(2010) 1350.
25. Jinghui Zhu, Dadamiah PMD Shaik, Hussain O .M., Yejun Qiu and Lei Zhao, *J. Electroanal. Chem*, (2017)
26. Q. Y. Liao, S. Y. Li, H. Cui and Chengxin Wang; *J. Mater. Chem. A*, 4(2016) 8830.
27. A. Bahloul, B. Nessark, E. Briot, H. Groult, A. Mauger, K. Zaghbi and C.M. Julien, *J. Power Sources* 240(2013) 267.
28. H. Song, X. luLin, Y. l. Zhang, H. Wang, H. yiLi and J. Huang, *Ceram. Int.*, 40(2014) 1251.
29. T. Zhou , Sh. Mo , Sh. Zhou , W. Zou , Y. Liu and D. Yuan, *J. Mater Sci* ,46(2011) 3337.
30. F. Zhang, X.G. Zhang, L. Hao, *Mater. Chem. Phys.*, 126(2011) 853.
31. C. H. Ng, H. N. Lim, Y. S. Lim, W. K. Chee and N. M. Huang, *Int. J. Energy Res.* (2014)
32. Y. Ren, J.Wang, X. Huang and J. Ding, *Electrochim. Acta*, 186(2015) 345.
33. W. Sun, L. Chen, Y. Wang, Y. Zhou, Sh. Meng, H. Li and Y. Luo, *Synth. React. Inorg. Met.-Org., Nano-Met. Chem.*, 46(2016) 437.
34. X. Zhang, X. Sun, Y. Chen, D. Zhang, Y. Ma, *Mater. Lett.*, 68 (2012) 336.
35. Z. Weixin, W. Cheng, Z. Xiaoming, X. Yi, and Q. Yitai, *Solid State Ionics*, 117(1999) 331.
36. A. Vazquez-Olmos, R. Redon, G. Rodriguez-Gattorno, *J. Colloid Interface Sci.*, 291(2005)175.
37. C. Nethravathi and M. Rajamathi, *Carbon*, 46(2008)1994.
38. Y. Liu, D. He, H. Wu, J. Duan, *Integrated Ferroelectrics*, 144(2013)118.
39. M. Zhu, R. Fu, *ADV Compos. Lett.*, 26(2017).